JOURNAL OF AIRCRAFT
Vol. 41, No. 5, September–October 2004

Probabilistic Two-Phase Aircraft Wake-Vortex Model: Application and Assessment

Frank Holzäpfel*
DLR, German Aerospace Center, 82234 Wessling, Germany
and
Robert E. Robins†
NorthWest Research Associates, Inc., Bellevue, Washington 98009-3027

Predictions of the parametric probabilistic two-phase aircraft wake-vortex transport and decay model P2P are compared with field observations. The two-phase decay model predicts probabilistic wake-vortex behavior as a function of aircraft and environmental parameters in real time. Observation data from field deployments accomplished at the International Airports Memphis and Dallas Fort Worth and from the WakeOP campaign performed at the airfield in Oberpfaffenhofen, Germany, are employed. In a scoring procedure, the predictive capabilities of a deterministic version of P2P are compared to Sarpkaya's model. Based on 211 Memphis cases, it is shown that the probabilistic model predicts conservative confidence intervals for vortex decay with the exception of four cases in which constant background wind shear increases vortex lifetime. Nonetheless, the aircraft spacing reduction potential based on vortex decay appears to be small. In contrast, consideration of advection outside the lateral limits of a safety corridor results in a large potential spacing reduction. Vortex drift is investigated based on input from different wind measurement devices with a focus on the spatial and temporal variability of the crosswind. Safety corridor clearances based on short-term weather forecasts yield promising results. Further, it is found that shear layers can modify vortex transport such that predicted uncertainty allowances are exceeded.

Nomenclature

A	=	constant
b	=	vortex spacing
C	=	constant to adjust turbulent spreading
g	=	gravitational acceleration
N	=	Brunt–Väisälä frequency
q	=	rms turbulence velocity
R	=	mean radius
r	=	radial coordinate
T	=	parameter for vortex age
t	=	time
U	=	horizontal wind velocity
u	=	axial velocity
v	=	lateral velocity
w	=	vertical velocity; descent speed
y	=	spanwise coordinate
z	=	vertical coordinate
Γ	=	circulation
ε	=	eddy dissipation rate
θ	=	potential temperature
Λ	=	one-half the longitudinal integral scale of atmospheric turbulence
ν	=	(effective) kinematic viscosity

Subscripts

0	=	initial value
1	=	first decay phase
2	=	second decay phase
5–15	=	average over circles with radii from 5 to 15 m
u	=	upper limit
y	=	lateral direction
z	=	vertical direction

Superscript

$*$	=	normalized quantity

Received 6 May 2003; presented as Paper 2003-3809 at the AIAA 21st Applied Aerodynamics Conference, Orlando, 23 June 2003; revision received 6 October 2003; accepted for publication 15 October 2003.

*Research Scientist, Institute of Atmospheric Physics, Oberpfaffenhofen; frank.holzaepfel@dlr.de.

†Research Scientist, P.O. Box 3027. Senior Member AIAA.

Introduction

AIRCRAFT-GENERATED wake vortices pose a potential risk for following aircraft. Mandated separation distances between consecutive aircraft that are meant to eliminate this risk unfortunately contribute significantly to the capacity constraints of major airports. However, experience and research results acquired over several decades have shown that wake-vortex separation standards might be overly conservative for a variety of meteorological situations.[1,2] Therefore, a parametric model that is capable of reliably predicting vortex positions and strengths in real time in a measured or forecasted atmospheric environment in the vicinity of the glide slope might be a useful tool for easing regulations without loss of safety.

Several parametric wake-vortex models that predict deterministic vortex behavior (see Refs. 3–6 for some of the better known models) are available. Not specified in these models are deviations from predicted values inherently caused by the stochastic nature of turbulence, complex vortex instabilities and deformations, and the uncertainty of environmental parameters that determine the vortices' behavior in the atmospheric boundary layer. The newly developed probabilistic two-phase wake-vortex transport and decay model P2P (Ref. 7) considers these deviations and predicts uncertainty allowances for vortex trajectories and vortex strength. The performance of a wake-vortex algorithm and, in particular, the size of the applied uncertainty allowances depend on the accuracy and variability of input parameters. Therefore, an assessment of wake-vortex model predictions must always consider the characteristics of the meteorological and wake-vortex observation systems.

Comparisons of wake-vortex prediction algorithms with observations are available in Refs. 8 and 9. Sensitivity studies on the impact of atmospheric conditions on a complete prototype wake-vortex

spacing system are given in Refs. 10 and 11. For this purpose either synthetic weather data[10] or the assumption that the observed environmental parameters persist for 30 min is used.[11]

In the current manuscript, P2P first is briefly introduced, and then an overview of the utilized databases is given. A deterministic version of P2P is compared to Sarpkaya's model[9] based on the statistics of 211 Memphis cases. The statistics of the Memphis cases are compared to 41 WakeOP cases, where environmental parameters are provided by different sensors and by a short-term weather forecast model system. The quality of vortex predictions is discussed with regard to the variability of environmental parameters. Probabilistic predictions are used to assess the performance of P2P and illustrate the significance of wind shear for vortex decay and transport. Finally, the aircraft spacing reduction potential based on vortex drift and decay is assessed.

Probabilistic Two-Phase Wake-Vortex Decay Model

A detailed description of P2P is given in Ref. 7. Here we restrict ourselves to an outline of the main properties of the model. P2P accounts for the effects of wind, turbulence, stable thermal stratification, and ground proximity where the interaction with the ground is modeled following the approach described in Ref. 8. Input data that characterize the wake vortices are time of vortex generation and initial position, circulation, and vortex spacing. Environmental input parameters are vertical profiles of crosswind, vertical wind, rms value of ambient turbulence, eddy dissipation rate (EDR), and potential temperature. The model is formulated in normalized form where the characteristic scales are based on initial vortex separation and circulation leading to the timescale $t_0 = 2\pi {b_0}^2/\Gamma_0$. EDR is normalized according to $\varepsilon^* = (\varepsilon b_0)^{1/3}/w_0$, where $w_0 = \Gamma_0/2\pi b_0$ denotes the initial descent speed, and temperature stratification is expressed by the normalized Brunt–Väisälä frequency $N^* = (g/\theta_0\, \mathrm{d}\theta/\mathrm{d}z)^{1/2} t_0$.

P2P employs a circulation Γ^*_{5-15}, which is averaged over circles with radii from 5 to 15 m or, alternatively, if smaller aircraft are considered, over a smaller radii interval. Γ^*_{5-15} combines several advantages for the evaluation of vortex strength from lidar data like the exclusion of small radii that are not reliably sensed by lidar, low sensitivity to observation angles, automatic compensation of vortex motion, and smoothing of scatter by averaging over several radii.[12] Moreover, Γ^*_{5-15} is well correlated with effects of potential wake encounters.[13]

The hydrodynamical basis of P2P relies on an equation that describes the spatiotemporal circulation evolution of the decaying potential vortex[14] for a given viscosity ν

$$\Gamma(r, t)/\Gamma_0 = 1 - \exp(-r^2/4\nu t) \tag{1}$$

From this relation the parameterizations of circulation decay and descent speed, which are "calibrated" based on large-eddy simulation (LES) data of different groups, are deduced.[15,16] The LES data suggest that the normalized circulation decays in two phases (see Fig. 1c). The diffusion phase described by part 1 of Eq. (2) is followed by a rapid decay phase[1,15,16] that can be parametrized by the full equation

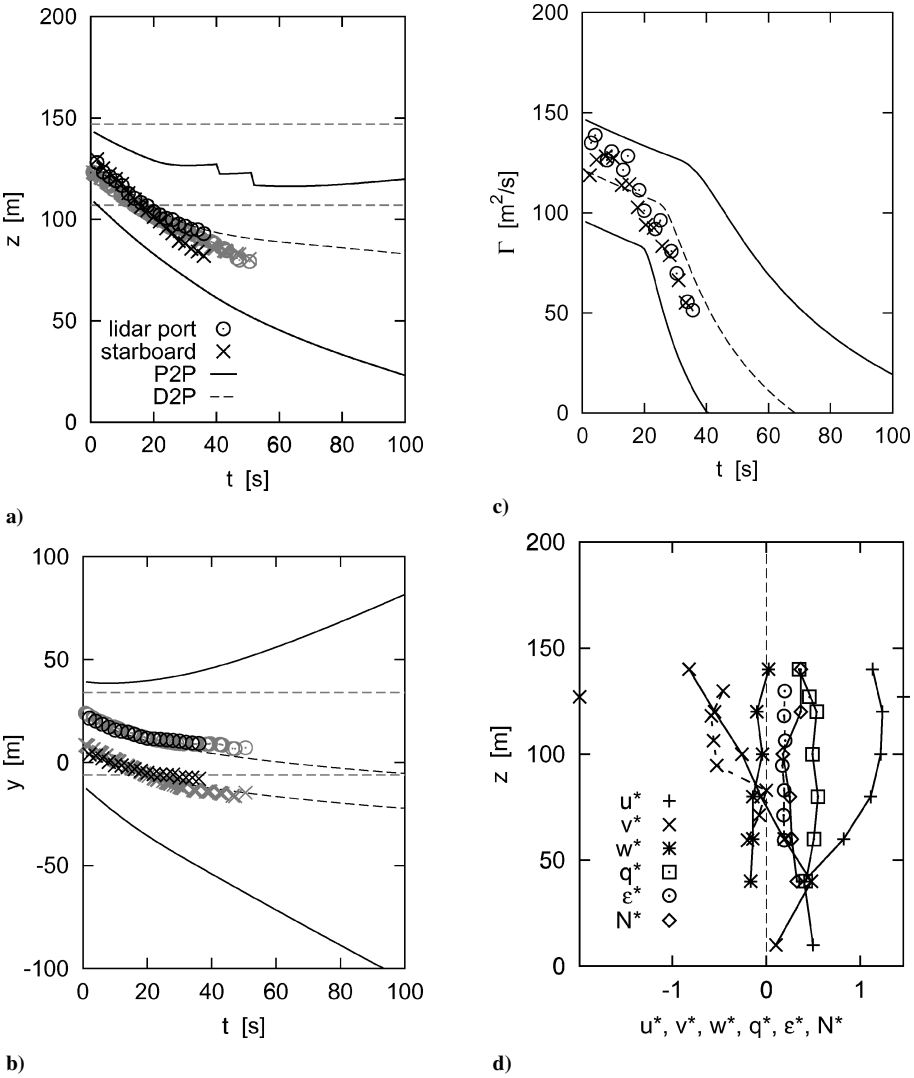

Fig. 1 Measured and predicted evolution of a) vertical and b) lateral positions and c) circulation of wake vortices from WakeOP flight 7-03 and d) vertical profiles of environmental data.

$$\Gamma^*_{5-15}(t^*) = \underbrace{A - \exp\frac{-R^2}{\nu_1^*\left(t^* - T_1^*\right)}}_{1} - \exp\frac{-R^2}{\nu_2^*\left(t^* - T_2^*\right)} \quad (2)$$

In Eq. (2) the onset time of rapid decay at T_2^* and the respective decay rate, which is adjusted by the effective viscosity ν_2^*, are functions of ambient turbulence and stratification. T_1^* and ν_1^* control decay in the diffusion phase, R corresponds to a mean radius, and A is a constant to adjust $\Gamma^*_{5-15}(t^* = 0)$. The descent rate obeys a nonlinear dependence on circulation, which allows for stagnating or even rebounding vortices with nonzero circulation in strongly stably stratified environments as observed in LES[15] and experiments.[17]

Precise deterministic wake-vortex predictions are not feasible operationally. Primarily, it is the nature of turbulence that deforms and transports the vortices in a stochastic way and leads to considerable spatiotemporal variations of vortex position and strength. Moreover, uncertainties of aircraft parameters and the variability of environmental conditions must be taken into account. Therefore, P2P is designed to predict wake-vortex behavior within defined confidence intervals.

In a first step, two consecutive runs of P2P with a variation of the decay parameters T_2^* and ν_2^* are performed. Second, constant uncertainty allowances of $\pm 0.2\Gamma_0^*$ for circulation and of plus and minus one initial vortex spacing for vertical and lateral locations are added. Finally, the increased scatter of vortices in turbulent environments is modeled by the assumption that the turbulence velocity acts as a superimposed propagation velocity.[18] An example of this applied to the upper bound of lateral position is

$$y_u^* = y^* + C_y \int q^*(z^*)\, \mathrm{d}t^* \quad (3)$$

where C_y is a constant of the order of one. Figure 1 depicts the resulting confidence intervals for a case where vortex evolution agrees well with the mean predictions.

Wake-Vortex Databases

The quality of wake vortex and coincident meteorological data and the conclusions that can be drawn from the data strongly depend on many factors including the measurement strategy, the type of sensors used, their locations, and the temporal and spatial resolution of the measurements, as well as the aircraft mix and the prevailing meteorological conditions. In the following we give an overview of the databases we have used to evaluate P2P. Because our investigations largely concentrate on Memphis and WakeOP data, a detailed description of the Dallas Fort Worth database is omitted.

Memphis

A detailed description of the wake-vortex field measurement campaign performed at Memphis International Airport during December 1994 and August 1995 is given in Refs. 19 and 20. We use data of 211 overflights measured at the Armory site, which was located 3 km south of the 36R runway touchdown zone where approaching aircraft were passing over at a height of nominally 150 m. The aircraft mix consisted of 81% medium and 19% heavy aircraft. The vortices were measured by a 10-μm continuous-wave lidar system with active tracking of the vortex range by real-time analysis of signal characteristics.

The meteorological instrumentation comprised various sensor systems including a 150-ft tower equipped with wind and temperature sensors on five different heights, a Doppler radar with a radio acoustic sounding system (RASS) option capable to measure wind and virtual temperature throughout the atmospheric boundary layer and a sodar to measure wind speeds in lower altitudes up to 400 m. The meteorological site was located at a distance of about 2 km from Armory. The wind velocity and temperature data arising from various sensors were merged to composite vertical profiles by human evaluators.

Eddy dissipation rate and turbulent kinetic energy (TKE) were derived from 30-min series of 10-Hz data measured on the instrumented tower at heights of 5 and 40 m. Vertical profiles of EDR and TKE were generated by applying similarity theory and scalings for the atmospheric boundary layer,[21] where the resulting profiles were required to match observations at a height of 40 m. The mean eddy dissipation rate fed into P2P predictions was $\overline{\varepsilon^*} = 0.083$ and varied between $0.0 \le \varepsilon^* \le 0.30$. The mean Brunt–Väisälä frequency was $\overline{N^*} = 0.21$ within bounds of $0 \le N^* \le 0.58$. Both turbulence and temperature stratification levels represent weak to moderate conditions.

WakeOP

The wake-vortex forecasting and measurement campaign WakeOP was conducted at the special airfield of Fairchild–Dornier in Oberpfaffenhofen, Germany, from 29 March to 4 May 2001. WakeOP has been accomplished in the framework of the Brite European research program C-Wake and the DLR project Wirbelschleppe. An outline of the campaign is given in Ref. 22. Figure 2 shows an airborne camera image of the WakeOP site with the flight track and the locations of the sensors from which data are obtained for the current study. The photo, which was shot with the high-resolution stereo camera—airborne extended, was provided by the DLR Institute WP. The 10-μm continuous-wave lidar systems of DLR, ONERA, and QinetiQ (locations denoted by l) were operated to trace the wake vortices generated by DLR's VFW 614 aircraft Advanced Technology and Testing Aircraft System (ATTAS). The ATTAS with a span of 21.5 m and an average weight of 18,000 kg performed overflights at a constant height of nominally 150 m above ground and produced wake vortices with a mean circulation of $\Gamma_0 = 142$ m^2/s and an average timescale of $t_0 = 12.6$ s. The flight tracks were defined according to the prevailing wind conditions to allow for simultaneous wake observations by the three lidars. Wake-vortex trajectories were determined with an accuracy of better than ± 4.0 m by triangulating the vortex core intersections of two simultaneously measuring lidars.[23] Based on vortex positions, circulation was determined as an average over a radii range from 3 to 8 m. For many overflights, doubly and triply sensed position and circulation data are available (see Fig. 1).

We compare the predictive capabilities of P2P based on four different sources of environmental data:

1) A mini-Sodar with a RASS extension provided vertical profiles of the three wind components, vertical fluctuation velocity, and virtual temperature. The vertical resolution was adjusted to 10 or 20 m and the averaging time to 10 min. Based on the assumption of isotropy, the rms value of turbulence was calculated from the vertical fluctuation velocity. The Brunt–Väisälä frequency was derived from the virtual temperature profiles.

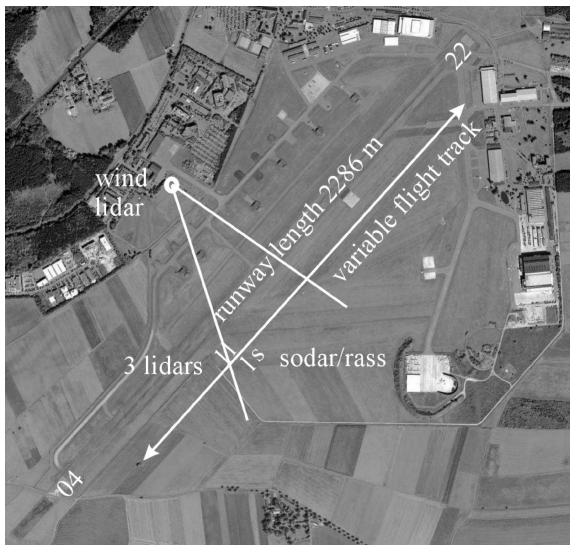

Fig. 2 WakeOP site, variable flight track, and locations of sensors.

2) A 2-μm pulsed Doppler wind lidar scanned under a constant elevation angle of 9 deg such that the measurement plane intersected the air volume in which the vortices evolved about 40 m below the flight track (see Fig. 2). From the line-of-sight wind measurements, which were performed for a period of 80 s after each overflight, vertical profiles of crosswind and eddy dissipation rate were deduced. The ε profiles were derived from the evaluation of the structure function in adjacent range bins[24] and averaged over several overflights.

3) The horizontal wind vector along the flight track was measured by the standard equipment of the ATTAS aircraft, which consists of the inertial aircraft navigation system and the airspeed system (pitot-static tube and resistence temperature sensor). The wind vector results from the difference of the vectors of ground velocity and wind velocity, where the latter arises from true airspeed and heading. The crosswind during the overflight was calculated as an average over a 10-s period. The particular time period of 10 s was chosen for the smoothing of the 5-Hz data to make sure that the data quality would correspond to operationally available AMDAR (aircraft meteorological data relay) data.[25] Furthermore, the turbulence velocity was derived from the rms value of crosswind fluctuations, which was determined from a 60-s crosswind record centered on the overflight time. Fluctuation quantities are not part of the AMDAR data set.

4) During the WakeOP campaign, the weather forecast model system NOWVIV[26] (now casting wake-vortex impact variables) predicted vertical profiles of wind velocities, virtual potential temperature, and turbulence velocity. NOWVIV was initialized every 12 h with output data from the operational weather forecast model LM of the German Weather Service. It was operated within a 2.1-km grid around the airfield with detailed terrain and land-use information and an increasing vertical spacing from 25 to 50 m throughout the boundary layer. The normalized eddy dissipation rate was derived from the predicted q profiles following Ref. 27 according to

$$\varepsilon^* = \tfrac{1}{2}(q/w_0)(b_0/\Lambda)^{\frac{1}{3}} \tag{4}$$

In Eq. (4) the one-half integral scale of atmospheric turbulence was set to the constant value of 110 m to avoid unrealistically large ε^* values caused by overestimated turbulence levels close to the ground. Deviations between measured and predicted normalized dissipation rates typically fell below 50%. Above the atmospheric boundary layer, the turbulence parameterization in NOWVIV tends to underestimate turbulence levels. As a consequence, the uncertainty allowances of P2P for lateral transport are rather small according to Eq. (3), which, in turn, increases the sensitivity on the predicted crosswind strength. Therefore, we assume that in low turbulent situations the minimum turbulence intensity of the wind amounts to 10%, and we estimate $q^*(z^*)$ according to

$$q^*(z^*) = \max[0.1|U^*(z^*)|, q^*(z^*)] \tag{5}$$

To ensure conservative predictions of vortex lifetime, we do not use the modified $q^*(z^*)$ values for the calculation of EDR in Eq. (4).

The current investigations are based on 41 overflights for which data from all described components are available. Figure 1 shows exemplarily a complete set of measured and predicted quantities for flight 3 on day 7 (flight # 7-03). In Figs. 1a–1c, the evolution of vertical and lateral positions and circulation of wake vortices against time as measured by two lidar pairings (grey and black symbols) and predicted by P2P (solid lines limit confidence intervals; dashed lines mark mean evolution) are depicted. P2P predictions are based on sodar/RASS data except ε^*, which is provided by Lidar, and the constants for turbulent spreading [see Eq. (3)] are set to $C_y = 1$, $C_z = 0.5$. A flight-path corridor is indicated by straight dashed lines. Figure 1d shows vertical profiles of the respective environmental data (sodar/RASS, solid lines; lidar, dashed lines; aircraft, symbols).

During the overflights, the mean value of the eddy dissipation rate used in P2P predictions was $\overline{\varepsilon^*} = 0.19$ and varied in an interval of $0.13 \le \varepsilon^* \le 0.25$. The mean Brunt–Väisälä frequency was $\overline{N^*} = 0.14$ within bounds of $0 \le N^* \le 0.44$. On average, the atmospheric conditions were more turbulent and less stably stratified in the WakeOP data than in the Memphis data.

Deterministic Model Performance

To evaluate the basic performance of the two-phase model, a deterministic version without probabilisitic components (termed D2P) is employed to predict mean vortex evolutions (compare Figs. 1a–1c, curved dashed lines), which are compared to predictions of the latest version of Sarpkaya's model.[9] For this purpose the 211 Memphis cases are used in a scoring procedure that is described in detail in Ref. 28. There, Sarpkaya's model, which is part of the current version of aircraft vortex spacing system (AVOSS),[29] was best rated compared to others.[6,8] The scoring procedure evaluates the rms deviations of measurement and prediction of the quantities $y^* = y/b_0$, $z^* = z/b_0$, and $\Gamma^*_{3-10} = \Gamma_{3-10}/\Gamma_0$ for each individual aircraft approach. From the resulting distribution of rms values, the median and the 90th percentile is used to characterize the performance of the models. In contrast to the original scoring procedure,[28] we consider the deviations of measurement and prediction for both vortices and every instant in time where measurements are available. In Ref. 28 statistics are computed only for the vortex having the greatest number of circulation observations, and predicted and observed values are interpolated onto the same uniform time grid.

The scoring results for the Memphis data are presented in Table 1. Although D2P was not designed to predict deterministic vortex behavior and although it was not adapted to the considered data basis in contrast to Sarpkaya's model[9] (decay constant C and effective vortex separation), the comparison is quite good. Note that in Table 1 and in Ref. 28 the calculated rms deviations of all of the investigated models are of similar magnitude. This indicates that major contributions to the rms deviations are probably caused by inconsistencies of the data basis as outlined next and by inherent deviations of wake evolution from deterministic model predictions.

Table 2 contains scoring results of the application of D2P to WakeOP data. The upper row displays the range of scoring results that is achieved when D2P is driven by various combinations of the available measurement data. For example, EDR can be taken from lidar and temperature, and vertical wind from sodar/RASS, and crosswind from ATTAS. In other D2P runs, only data available from one device are used, and the remaining parameters are set to zero. The intervals in Table 2 are also achieved when only aircraft crosswind information is used and D2P assumes the baseline decay and descent rates parameterized for $\varepsilon^* = N^* = 0$. Further, the intervals achieved by a single model, which is driven by different environmental input (upper row of Table 2), even exceed the variations found for the different wake-vortex models applied to the Memphis data (compare Table 1). This finding clearly points up the importance of high-quality environmental data. The D2P rating based on the NOWVIV short-term weather forecasts depicted in the lower row yields remarkably good results. With the exception of lateral transport, the results are well within the range of D2P predictions based on measurements.

On average, the scoring results of WakeOP are better than for Memphis. This can result from several factors. Potentially, the

Table 1 Statistics for normalized differences between deterministic model predictions and 1995 observations from Memphis International Airport

Model	Averages	rms Δy^*	rms Δz^*	rms $\Delta\Gamma^*$
Sarpkaya's	Median	0.776	0.436	0.156
	90th perc.	2.33	0.912	0.276
D2P	Median	0.783	0.427	0.187
	90th perc.	2.26	0.898	0.310

Table 2 Statistics for normalized differences between D2P predictions and observations from WakeOP campaign

Meteo input	Averages	rms Δy^*	rms Δz^*	rms $\Delta\Gamma^*$
Sodar/RASS,	Median	0.663–0.753	0.384–0.444	0.145–0.156
lidar, aircraft	90th perc.	1.32–2.17	0.804–1.09	0.208–0.264
NOWVIV	Median	1.12	0.402	0.155
	90th perc.	2.23	0.803	0.239

triangulation strategy[23] has increased the accuracy of lidar data. However, it is probably the immediate proximity of the meteorological sensors to the wake measurement site that explains the superior results regarding lateral transport. On the other hand, the observation times with an average of $\overline{t^*} = 2.7$ were shorter in WakeOP than in Memphis with $\overline{t^*} = 3.8$, with the result that the Memphis predictions have more time to deviate from observations. The shorter durations are caused by the fact that for triangulation two lidars must observe the vortices simultaneously and the intersection of two observation domains is always smaller than the observation domain of a single lidar. Finally, during the WakeOP campaign turbulence levels were higher, which also can reduce observation times but, conversely, can also degrade model performance.

Another remarkable conclusion can be drawn from a comparison of the scoring results for lateral transport based on Memphis measurements and on WakeOP short-term weather forecasts (NOWVIV). The 90th-percentile deviations, which are of high operational relevance because they represent the poorly predicted cases, yield the almost identical values of 2.26 and 2.23 for lateral transport. This result indicates that the magnitude of the forecast error of crosswind roughly corresponds to the spatial variability of the crosswind over a distance of 2 km. The 2-km distance corresponds to the separation between the Memphis sites for wind and wake-vortex data acquisition. This suggests that instantaneous measurement data of a costly 2-km spaced grid of wind measurement instrumentation along the glide path would not yield much superior results compared to a numerical prediction scheme without assimilation of local instrumentation data. Note that this conclusion is preliminary because it is based on a statistically insufficient amount of data. Further, it neglects the impact of the differences just listed between the Memphis and WakeOP data, and, in particular, it assumes that measurement errors can be neglected.

A closer inspection of how the choice of the device that is used for the determination of crosswind affects the performance of D2P is given in Fig. 3. The figure shows statistics for normalized differences between predictions and observations of lateral wake vortex transport based on different sources of crosswind data for 41 WakeOP cases. Results from the Memphis database are included for comparison. The ratings based on lidar crosswind measurements yield the least dispersed results. Possibly, the averaging time of 80 s is most appropriate because it corresponds roughly to the life span of the vortices. Although the lowest median values are reached with sodar and aircraft data, the respective high 90th-percentile values reflect the suboptimal averaging times of 10 min and 10 s, respectively.

The strong significance of temporal and spatial averaging intervals is best illustrated by the wind inhomogenities, which were observed along the flight track of overflight 8-16 (Fig. 4a). A crosswind jump of almost 5 m/s along less than 200-m length of flight track is advected into the measurement domain in less than 60 s by an

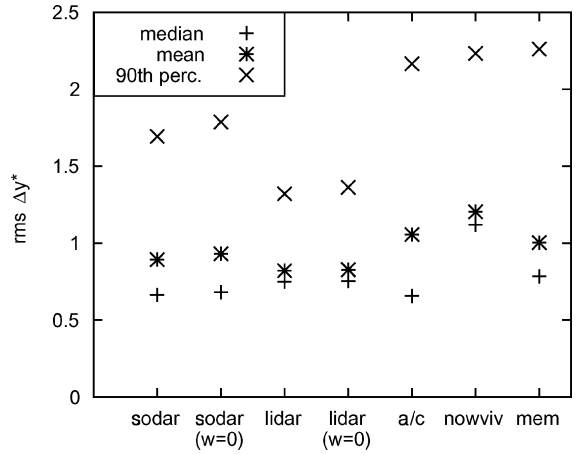

Fig. 3 Statistics for normalized differences between predictions and observations of lateral wake-vortex transport based on different sources of crosswind data.

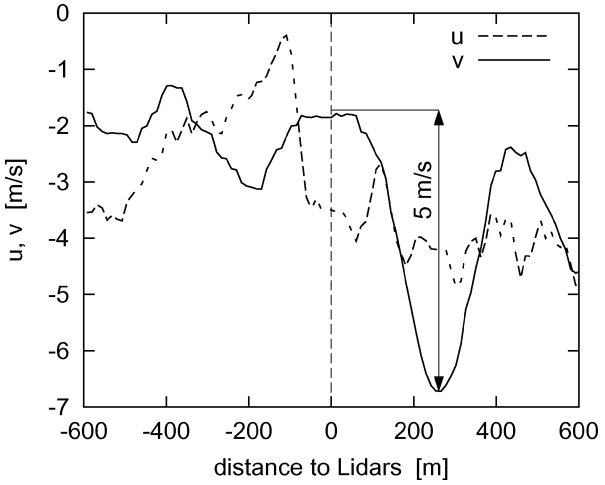

Fig. 4a Axial wind and crosswind along ATTAS flight track.

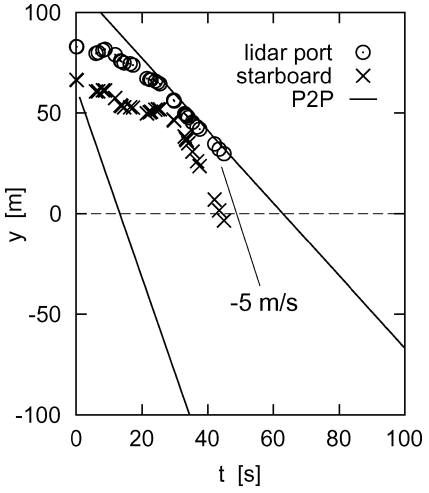

Fig. 4b Associated lateral vortex drift measured by lidar and predicted by P2P.

axial wind of about −3 m/s. This is evidenced by the strong lateral acceleration of the vortices delineated in Fig. 4b (line indicates a lateral drift velocity of $v = -5$ m/s). It is most obvious that deterministic wake-vortex predictions must fail here, whereas P2P (based on aircraft wind data) just manages to predict the confidence intervals correctly. P2P predictions driven by sodar and lidar crosswinds yield adequate confidence intervals as a result of the high level of measured turbulence, whereas the lower turbulence predicted by NOWVIV causes insufficient uncertainty allowances (not shown).

Tables 1 and 2 indicate that the deviations of measurement and prediction for lateral transport are roughly doubled compared to vertical transport. This reflects the larger variability and sensitivity associated with crosswind transport compared to the impact of the parameters turbulence, stratification, and vertical wind that control vortex descent. Therefore, for probabilistic predictions we adjust the constants for turbulent spreading to $C_y = 1$ and $C_z = 0.5$.

Finally, Fig. 3 indicates that the exclusion of vertical wind measurements ($w = 0$) can degrade results. Obviously, a more precise temporal descent history along vertical crosswind profiles seems to affect lateral transport favorably. Conversely, we observed situations where the sodar measured positive vertical winds in an updraft, whereas the vortices in immediate proximity of the sodar site experienced negative winds. This means that at least in convective situations, where solar radiation drives the formation of updrafts that are connected to adjacent downdraft regions and both updrafts and downdrafts have extensions that can transport substantial parts of wake vortices in opposite directions,[18] signed vertical wind velocities should not enter the predictions of vertical vortex transport.

In convective atmospheric boundary layers it could be beneficial to use the magnitude of vertical wind velocities to increase vertical uncertainty allowances.

Probabilistic Model Performance and Aircraft Spacing Reduction Potential

The probabilistic model performance cannot be evaluated by the preceding used scoring approach because increased uncertainty allowances would always improve ratings. Therefore, in this section the probability that the vortices actually evolve within predicted confidence intervals is discussed with regard to a potential runway capacity gain. For an operational system, the uncertainty allowances must be adjusted such that they meet accepted probabilities of appropriate risk metrics. This is beyond the scope of the current manuscript.

The investigations concerning wake-vortex decay are restricted to the Memphis data because there the durations of vortex measurements were generally longer. Vortex transport is considered based on WakeOP data because there vortex trajectory data evaluated by triangulation and a variety of crosswind data sources are available.

Decay

From the 211 investigated Memphis cases, P2P underestimates circulation for only 0.75% of the measurements provided that the operationally irrelevant initial overestimation of circulation by lidar (compare Fig. 5c) is neglected. In Ref. 12 it is demonstrated that initial overestimations of root circulation by 30–70% can occur when a radii-averaging circulation definition like Γ^*_{5-15} is applied. Radii-averaging methods interpret line-of-sight velocities of secondary vortices, which are induced for example by the edges of a flap, as high tangential velocities on large radii of the primary vortex, hence, high circulation. The overestimation ceases when the roll-up process of the multiple vortices that evolve behind an aircraft in high-lift configuration to a single vortex pair is completed.

Rejecting further obviously erroneous measurements, four slightly nonconservative cases (1150, 1151, 1267, 1273) remain. Figure 5 shows case 1150 (B727 aircraft) in detail. The longevity of the vortices in these four cases most likely is caused by shear-layer effects caused by nocturnal low-level jets. All four cases were measured around midnight in a quite stably stratified and low turbulent environment. And in all four cases an unusually long-lived and stalling vortex is observed.

Unfortunately, the crosswind profiles provided by the human evaluator (fine crosses in Fig. 5d) did not result in the observed lateral vortex drift (compare grey dashed lines with symbols in Fig. 5b), but reliable crosswind profiles (bold crosses connected by lines, Fig. 5d) that yield good agreement with the observed vortex drift (black dashed lines, Fig. 5b) could be reconstructed from the measured sodar and tower data. The reconstructed vertical wind profiles

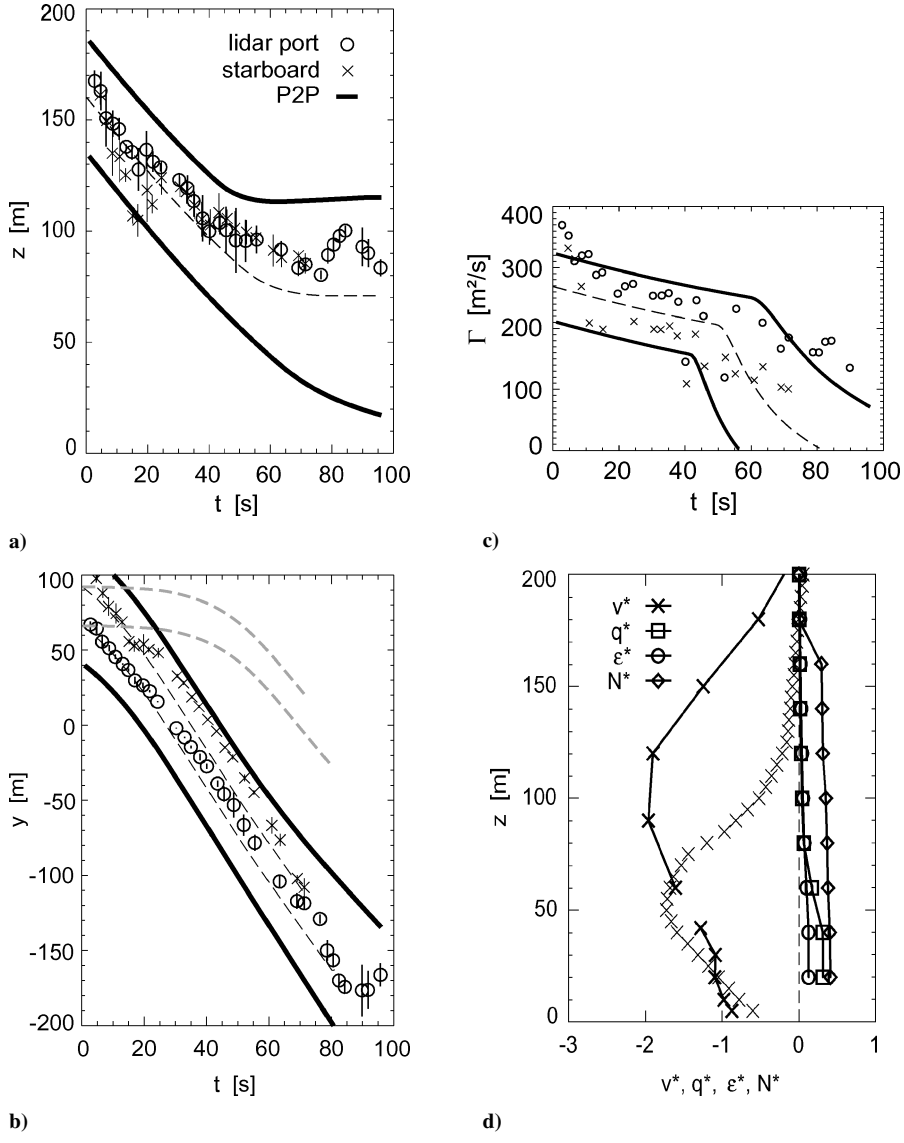

Fig. 5 a–c) Comparison of P2P predictions with lidar observations for Memphis case 1150 and d) vertical profiles of environmental data.

contain considerable shear, and in all four cases it is the vortex with the same signed vorticity (SSV vortex) as the vorticity of the background shear that persists longer than its partner vortex by one to three time units.

The fact that for given turbulence the decay of the SSV vortex can be retarded in a constantly sheared environment (compared to the nonsheared environment) is elucidated by numerical simulations,[30,31] which show that vertical shear of $\partial v^*/\partial z^* = 1$ can enhance vortex lifetime by one to two timescales. The shear intensity $\partial v^*/\partial z^* = 1$ represents the case where the background shear just compensates the shear that one vortex excerts on its partner. As a consequence, the destructive effects of mutual strain do not apply for one of the vortices. Further, it can be shown that for the SSV vortex the formation of spiral-shaped secondary vorticity structures, which play a crucial role for vortex decay, is strongly delayed.[32] In case 1150, we determine that there is vertical shear of $\partial v^*/\partial z^* = 0.6$ prevailing in a height interval of 120–180 m. This shear strength seems to be sufficient to reduce the descent and to increase the life span of the SSV vortex noticeably.

Our experience suggests that the complex wake-vortex shear-layer interaction cannot be predicted reliably in an operational environment, in particular because of the difficulties related to the observation and prediction of shear-layer profiles. Therefore, situations where shear-layer effects are not covered by uncertainty allowances have to be identified, and reduced spacing operations based on vortex decay must be ruled out.

Based on the assumption that P2P is capable of predicting upper bounds of the circulation evolution, the respective aircraft spacing reduction potential is assessed. Figure 6 delineates the cumulative distributions of aircraft separations that result from decay predictions of P2P for over 400 cases when an arbitrarily chosen threshold of $\Gamma_t = 100$ m^2/s for acceptable vortex strengths is applied. For international civil aviation organization (ICAO) separations (grey bars) a medium approach speed of 70 m/s is assumed. In addition to the 211 Memphis cases, another 191 cases from the 1997 Dallas Fort Worth deployment[33] are included, which lead to similar results. The comparison of the predicted aircraft separations to the currently effective ICAO separations clearly indicates that conservative decay predictions do not allow for reduced spacing. In the majority of the cases, durations predicted by P2P exceed ICAO standards significantly. Reasonably modified circulation threshold values do not alter this statement.

In another study[34] it is found that in 45% of 346 Memphis cases lidar wake-vortex detection times exceed ICAO separations for heavy–heavy aircraft pairings, where the mean circulation at the respective separation of 4 n miles amounts to 0.42 Γ_0. These findings clearly indicate that it is mainly the transport of vortices away from the glide path by descent and/or advection by crosswind, which is responsible for the high level of safety provided by the currently effective aircraft separation standards. Consequently, these results suggest that in many cases only transport bears the potential to allow for reduced spacing operations with appreciable capacity benefits.

Transport

We use the 41 WakeOP cases to evaluate the potential of P2P to predict the time when the vortices have left a safety corridor around the flight track based on different crosswind data sources. The dimensions of the safety corridor are taken from an evaluation of the navigational performance of instrumental landing system (ILS) approaches at Frankfurt International Airport,[35] which is based on 40,000 approaches collected by radar. For the nominal flight altitude of the ATTAS aircraft of 150 m, 95% (2σ) of the aircraft deviated less than 20 m in lateral and vertical direction from the ILS. Therefore, we define a safety corridor with ± 20 m in both directions.

In addition to the safety corridor and the uncertainty allowances predicted by P2P, another allowance is needed that considers the dimensions of the hazard area around the vortex center position.[36,37] The dimensions of the hazard area depend on the pairing of vortex-generating and following aircraft, the degree of vortex decay, and generally accepted metrics for a safe encounter. In a future operational system, P2P and the dynamically determined dimensions of the hazard area predicted by the DLR Simplified Hazard Area Prediction (SHAPe) model will be linked. The idea is that during one prediction cycle the hazard area shrinks such that aircraft separations can be adjusted to the time when either the hazard area has left the safety corridor or has vanished. Rossow[37] suggests a conservative and static hazard area that can be represented by two wing spans of the wake-generating aircraft in breadth and one wing span in height. This definition corresponds to an one half-span allowance that is added to the vortex center positions in lateral and vertical directions. Because the SHAPe model is still under development, we first neglect the hazard area and then employ the static definition.

Figure 7 shows the cumulative distributions of the vortex ages at which the vortices have left the safety corridor in lateral direction based on lidar observations and P2P predictions. For these predictions P2P employs crosswind data provided either by sodar, lidar, aircraft, or NOWVIV. Table 3 delineates respective quantities that characterize the efficiency of the different approaches. In 76% of the lidar observations, the vortices leave the safety corridor. In the remaining cases, the vortices either stay and decay within the lateral bounds of the corridor, or the observations cease before the vortices could leave the corridor (compare Fig. 1). In P2P predictions, the time to leave the corridor is delayed, and only a reduced fraction of the vortices leave the corridor. This conservative character of the predictions is directly related to the fact that P2P predicts confidence intervals, whereas lidar observations represent two particular vortex

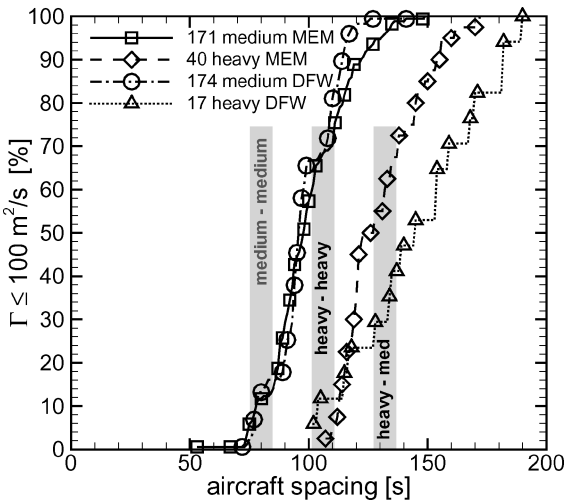

Fig. 6 Aircraft separations based on conservative decay predictions of P2P.

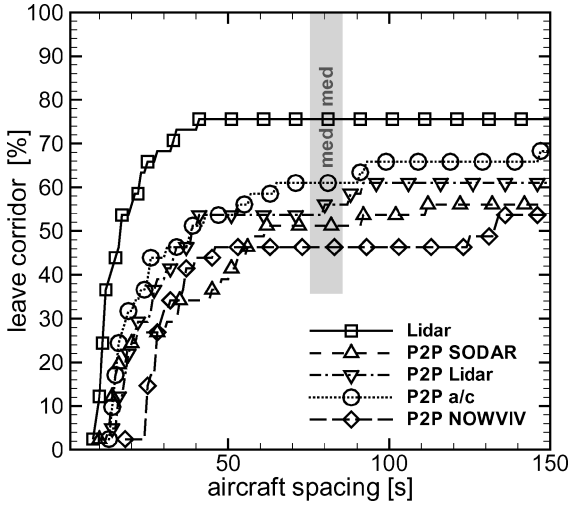

Fig. 7 Cumulative distributions of times to leave the safety corridor in lateral direction.

trajectories. The measured average corridor occupation time for the vortices that leave the corridor amounts to 17 s (Table 3). Although this time on average is more than doubled in P2P predictions, there is still potential for appreciable capacity benefits.

Depending on the crosswind source, P2P generates zero to three nonconservative predictions (NoCoPs). NoCoPs denote cases where according to P2P the corridor is cleared from vortices by lateral transport, whereas lidar measurements indicate that there are still vortices inside the corridor. In the investigated cases, the vortices leave the corridor only a few seconds after the predicted clearance. However, all NoCoPs represent nonhazardous situations because the vortices have descended below the corridor floor in advance of the predicted lateral escape. NoCoPs can be entirely avoided when the constant for spreading of the confidence intervals [see Eq. (3)] is increased from $C_y = 1$ to 3.5 for predictions based on lidar and aircraft crosswind data and to $C_y = 1.5$ for crosswind provided by NOWVIV. The percentage of vortices that leave the corridor then decreases to 10, 37, and 46% with average corridor occupation times of 46, 33, and 46 s, respectively.

Table 3 Efficiency of lateral transport for 41 WakeOP cases based on different crosswind data sources

Method	Leave corridor, %	ACOT time, s	NoCoPs, –
Observation	76 (76)	17 (20)	——
P2P fed with crosswind from:			
SODAR	56 (56)	37 (46)	0 (0)
Lidar	61 (61)	32 (39)	1 (1)
Aircraft	68 (66)	35 (38)	3 (2)
NOWVIV	54 (46)	44 (39)	1 (0)

Table 3 shows further that the efficiency of the approach is only slightly reduced when the static hazard area definition is applied (numbers in brackets). For the ATTAS aircraft, the hazard area is represented by the one half-span length of 10.75 m, which is added to the predicted uncertainty allowances. The introduction of the hazard area either slightly decreases the number of vortices that leave the corridor or it slightly increases the corridor occupation time. The number of NoCoPs remains equal or decreases. Note that the prediction chain NOWVIV-P2P still allows for reduced separations in 46% of the cases with an average corridor occupation time of 39 s and without any NoCoP.

Figure 8 shows the wake evolution of WakeOP overflight 7-08, where wind shear effects modify vortex descent and lateral transport such that the uncertainty allowances of P2P are slightly exceeded. The grey symbols in Figs. 8a and 8b indicate that the vortices start to tilt at a height of 100 m and finally reach a maximum tilt angle of 53 deg. Whereas the port vortex continues to descend undamped, the starboard vortex is stalling at a height of 75 m. At the same time the vortex spacing is increased to a maximum of 2.2 b_0. It is not perceptible to what extent the deviation of lateral transport from pure advection is caused by the mutually induced lateral velocity of the tilted vortex pair or the mutual velocity induction of the aircraft vortices with the vorticity patches that are released from the shear layer. Anyway, the described effects are consistent with the topology of wake vortex interaction with shear layers shown by numerical

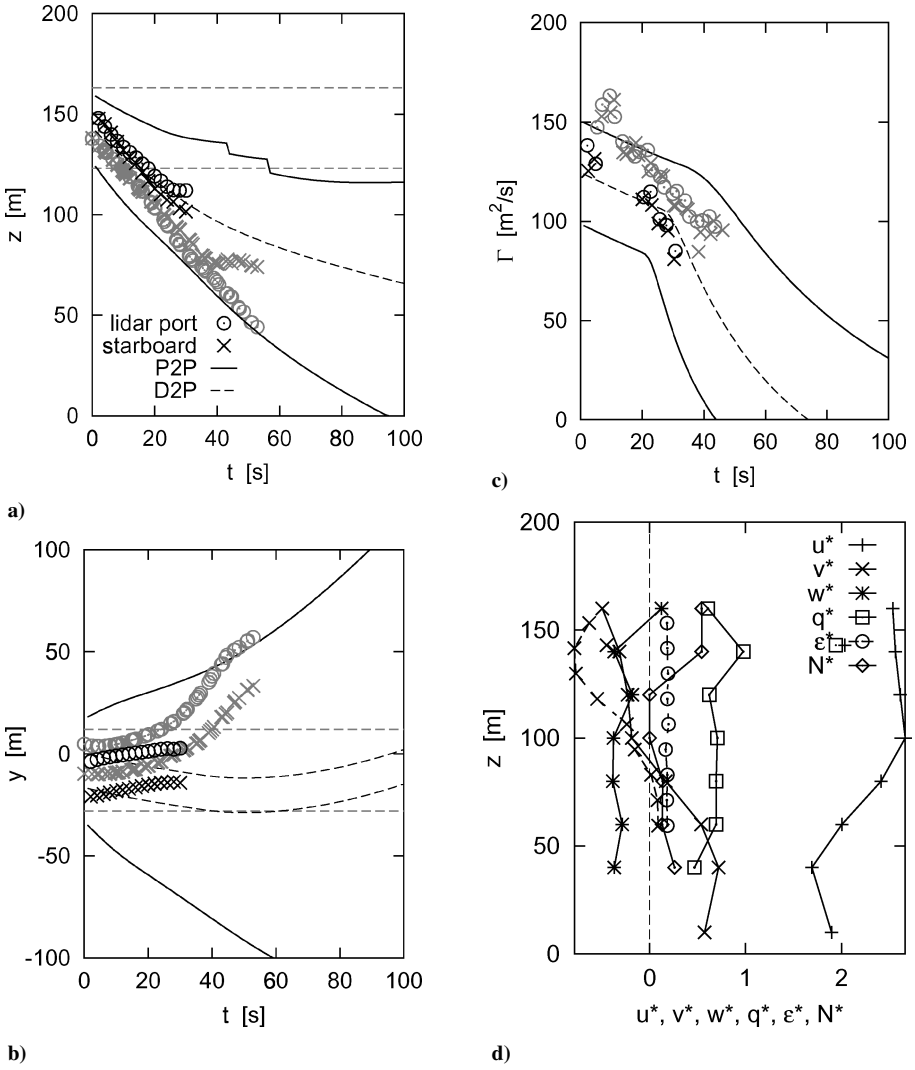

Fig. 8 Wake evolution of WakeOP overflight 7-08. Detailed description given in WakeOP section.

simulations.[30,31] We note that compared to the shear assumed in the simulations the maximum normalized shear of 0.3–0.4 measured by lidar and sodar is not very strong. Note that also the axial wind component contains shear of a similar strength.

The different signs of measured and predicted initial lateral drift directions in Fig. 8b indicate that there was considerable variability in the windfield and that potentially higher shear rates could have prevailed in the vicinity of the vortices. This example highlights that shear effects can cause the exceedance of the predicted uncertainty allowances not only regarding decay (see the preceding) but also regarding transport. Further, it illustrates that sufficiently precise observations and, in particular, predictions of shear-layer characteristics are hardly feasible. Even with the applied dedicated wind measurement devices it was not possible to measure shear layers with sufficient accuracy to fully explain the observed vortex behavior. As a consequence, a tradeoff between wind shear prediction capabilities and appropriate uncertainty allowances weighted by the probability of respective shear layers will have to be found.

The relatively small absolute descent distance of the vortices generated by the ATTAS aircraft prevents a meaningful discussion of the potential to reduce aircraft separations based on vortex descent. Although lidar observations indicate an average corridor occupation time of 18 s for 90% of the overflights, it turns out that for aircraft of relatively small size (ATTAS falls towards the lower end of the medium-size category) the upper boundary of the predicted confidence interval often resides close to the boundary of the safety corridor (see Figs. 1a and 8a). As a consequence, already minor modifications of parameters modify statistics significantly such that the results can hardly be transfered to the typical aircraft mix prevailing at large airports.

Conclusions

The probabilistic two-phase wake-vortex model P2P was applied to observed data from three different field deployments. Altogether, the performance of P2P proves a high level of skill, and the uncertainty allowances appear appropriate. Furthermore, the comparison of a deterministic version of P2P to Sarpkaya's model[9] yields good results. Naturally, the assessment of P2P was done based on a limited number of cases representing only segments of the real weather conditions over which it must finally operate. Therefore, further analyses must complement the current investigations.

Predictions of lateral vortex drift based on different crosswind data sources elucidate the significance of the spatiotemporal wind variability. This variability clearly illustrates the need of probabilistic wake-vortex modeling and the necessity to apply appropriate spatiotemporal resolution in the observations of environmental parameters. It is found that the uncertainties connected with 2-km separated wind observations are of the same order as uncertainties connected to short-term weather forecasts. This result, however, is based on a statistically insufficient amount of data. For vortex descent, uncertainties are noticeably lower. Therefore, we halve the constants for vertical turbulent spreading.

In the majority of the cases, the probabilistic predictions of P2P are conservative. Only flawed crosswind information or pronounced wind shear can cause deficient predictions. Detailed investigations of individual cases reveal that constant wind shear can prolong vortex lifetime, whereas shear layers can modify vertical and lateral transport. These findings corroborate results of numerical simulations.[30,31] Increased uncertainty allowances could eliminate erroneous predictions at the expense of a decreased aircraft spacing reduction potential. Further analyses of observation data are needed to find optimum uncertainty allowances that permit the increase of airport capacity without loss of safety. Apparently, uncertainty allowances are site specific and depend heavily on the available equipment and its performance.

Our investigations indicate that vortex decay proceeds too slowly for appreciable capacity benefits, whereas lateral vortex drift bears considerable potential for safe reduced spacing operations. Clearly, the quality of crosswind measurements and forecasts determines the efficiency of the approach. With regard to the considerable observed crosswind variability, this remains a challenging venture. Almost surprisingly, crosswind provided by short-term weather forecasts would have allowed the safe reduction of separations to below 50 s in 39% of the WakeOP cases. However, this assessment relies on a single control window along the flight path.

A future goal would be to improve short-term weather forecasts by the assimilation of local weather observations. P2P predictions based on now casted environmental parameters could allow for medium-term scheduling applications. Reduced aircraft separations would only be applied provided that current weather observations match weather predictions.

Acknowledgments

We gratefully acknowledge the essential contributions of all of the teams during the WakeOP trial and the subsequent data processing. The WakeOP campaign has been carried out in the framework of the Brite European research program C-Wake under Contract No. GRD1-1999-10332 and the DLR project Wirbelschleppe. The distribution of the Memphis and Dallas Fort Worth databases by the NASA Langley Research Center, Hampton, Virginia, is greatly appreciated.

References

[1]Gerz, T., Holzäpfel, F., and Darracq, D., "Commercial Aircraft Wake Vortices," *Progress in Aerospace Sciences*, Vol. 38, No. 3, 2002, pp. 181–208.

[2]Hallock, J. N., Greene, G. C., and Burnham, D. C., "Wake Vortex Research—a Retrospective Look," *Air Traffic Control Quarterly*, Vol. 6, No. 3, 1998, pp. 161–178.

[3]Greene, G. C., "An Approximate Model of Vortex Decay in the Atmosphere," *Journal of Aircraft*, Vol. 23, No. 7, 1986, pp. 566–573.

[4]Corjon, A., and Poinsot, T., "Vortex Model to Define Safe Aircraft Separation Standards," *Journal of Aircraft*, Vol. 33, No. 3, 1996, pp. 547–553.

[5]Sarpkaya, T., "New Model for Vortex Decay in the Atmosphere," *Journal of Aircraft*, Vol. 37, No. 1, 2000, pp. 53–61.

[6]Jackson, W., Yaras, M., Harvey, J., Winckelmans, G., Fournier, G., and Belotserkovsky, A., "Wake Vortex Prediction—An Overview," Transport Canada, Rept. TP 13629E, Montreal, March 2001.

[7]Holzäpfel, F., "Probabilistic Two-Phase Wake Vortex Decay and Transport Model," *Journal of Aircraft*, Vol. 40, No. 2, 2003, pp. 323–331.

[8]Robins, R. E., Delisi, D. P., and Greene, G. C., "Algorithm for Prediction of Trailing Vortex Evolution," *Journal of Aircraft*, Vol. 38, No. 5, 2001, pp. 911–917.

[9]Sarpkaya, T., Robins, R. E., and Delisi, D. P., "Wake-Vortex Eddy-Dissipation Model Predictions Compared with Observations," *Journal of Aircraft*, Vol. 38, No. 4, 2001, pp. 687–692.

[10]Riddick, S. E., and Hinton, D. A., "An Initial Study of the Sensitivity of Aircraft Vortex Spacing System (AVOSS) Spacing Sensitivity to Weather and Configuration Input Parameters," NASA/TM-2000-209849, Jan. 2000.

[11]Rutishauser, D. K., and O'Connor, C. J., "Aircraft Vortex Spacing System (AVOSS) Performance Update and Validation Study," NASA/TM-2001-211240, Oct. 2001.

[12]Holzäpfel, F., Gerz, T., Köpp, F., Stumpf, E., Harris, M., Young, R. I., and Dolfi-Bouteyre, A., "Strategies for Circulation Evaluation of Aircraft Wake Vortices Measured by Lidar," *Journal of Atmospheric and Oceanic Technology*, Vol. 20, No. 8, 2003, pp. 1183–1195.

[13]Hinton, D. A., and Tatnall, C. R., "A Candidate Wake Vortex Strength Definition for Application to the NASA Aircraft Vortex Spacing System (AVOSS)," NASA TM 110343, Sept. 1997.

[14]Zierep, J., *Ähnlichkeitsgesetze und Modellregeln der Strömungslehre*, Braun, Karlsruhe, Germany, 1982, pp. 69–72.

[15]Holzäpfel, F., Gerz, T., and Baumann, R., "The Turbulent Decay of Trailing Vortex Pairs in Stably Stratified Environments," *Aerospace Science and Technology*, Vol. 5, No. 2, 2001, pp. 95–108.

[16]Proctor, F. H., and Switzer, G. F., "Numerical Simulation of Aircraft Trailing Vortices," *Proceedings of the 9th Conference on Aviation, Range and Aerospace Meteorology*, Paper 7.12, American Meteorological Society, Boston, Sept. 2000.

[17]Sarpkaya, T., "Trailing Vortices in Homogeneous and Density-Stratified Media," *Journal of Fluid Mechanics*, Vol. 136, 1983, pp. 85–109.

[18]Frech, M., and Holzäpfel, F., "A Probabilistic Prediction Scheme for Wake Vortex Evolution in a Convective Boundary Layer," *Air Traffic Control Quarterly*, Vol. 10, No. 1, 2002, pp. 23–41.

[19]Dasey, T. J., Campbell, S. D., Heinrichs, R. M., Matthews, M. P., Freehart, R. E., Perras, G. H., and Salamitou, P., "A Comprehensive System for Measuring Wake Vortex Behavior and Related Atmospheric Conditions at Memphis, Tennessee," *Air Traffic Control Quarterly*, Vol. 5, No. 1, 1997, pp. 49–68.

[20]Campbell, S. D., Dasey, T. J., Freehart, R. E., Heinrichs, R. M., Matthews, M. P., Perras, G. H., and Rowe, G. S., "Wake Vortex Field Measurement Program at Memphis, TN, Data Guide," Lincoln Lab., Project Rep. NASA/L-2, Massachusetts Inst. of Technology, Cambridge, MA, Jan. 1997.

[21]Han, J., Arya, S. P., Shen, S., and Lin, Y.-L., "An Estimation of Turbulent Kinetic Energy and Energy Dissiptaion Rate Based on Atmospheric Boundary Layer Similarity Theory," NASA/CR-2000-210298, June 2000.

[22]Gerz, T., "Wake Vortex Prediction and Observation: Towards an Operational System," *Proceedings of the 3rd ONERA–DLR Aerospace Symposium*, 2001, Chap. S1-3.

[23]Köpp, F., Smalikho, I., Rahm, S., Dolfi, A., Cariou, J.-P., Harris, M., Young, R. I., Weekes, K., and Gordon, N., "Characterisation of Aircraft Wake Vortices by Multiple-Lidar Triangulation," *AIAA Journal*, Vol. 41, No. 6, 2003, pp. 1081–1088.

[24]Banakh, V. A., and Smalikho, I. N., "Estimation of the Turbulent Energy Dissipation Rate from the Pulsed Doppler Lidar Data," *Atmospheric and Oceanic Optics*, Vol. 10, No. 12, 1997, pp. 957–965.

[25]Painting, D., *AMDAR Reference Manual*, WMO-No. 958, World Meteorological Organisation, Geneva, 2003, p. 24.

[26]Frech, M., and Tafferner, A., "The Performance of the Model System NOWVIV During the Field Campaign WakeOP," *Proceedings of the 10th Conference on Aviation, Range and Aerospace Meteorology*, Paper J7.4, American Meteorological Society, Boston, May 2002.

[27]Donaldson, C. duP., and Bilanin, A. J., "Vortex Wakes of Conventional Aircraft," NATO, AGARD, AG-204, Paris, May 1975.

[28]Robins, R. E., and Delisi, D. P., "Wake Vortex Algorithm Scoring Results," NASA/CR-2002-211745, June 2002.

[29]Hinton, D. A., "An Aircraft Vortex Spacing System (AVOSS) for Dynamical Wake Vortex Spacing Criteria," *The Characterization and Modification of Wakes from Lifting Vehicles in Fluids*, AGARD, Neuilly-sur-Seine, France, 1996, pp. 23.1–23.11.

[30]Hofbauer, T., "Numerische Untersuchungen zum Einfluss von Windscherung und Turbulenz auf Flugzeugwirbelschleppen," Deutsches Zentrum für Luft- und Raumfahrt, Forschungsbericht 2003-01, Inst. für Physik der Atmosphäre, Oberpfaffenhofen, Germany, 2003.

[31]Hofbauer, T., and Holzäpfel, F., "Behavior of Aircraft Wake Vortices Subjected to Wind Shear," AIAA Paper 2003-3813, June 2003.

[32]Holzäpfel, F., Hofbauer, T., Darracq, D., Moet, H., Garnier, F., and Ferreira Gago, C., "Analysis of Wake Vortex Decay Mechanisms in the Atmosphere," *Aerospace Science and Technology*, Vol. 7, No. 4, 2003, pp. 263–275.

[33]Dasey, T. J., Cole, R. E., Heinrichs, R. M., Matthews, M. P., and Perras, G. H., "Aircraft Vortex Spacing System (AVOSS) Initial 1997 System Deployment at Dallas/Ft. Worth (DFW) Airport," Lincoln Lab., Project Rep. NASA/L-3, Massachusetts Inst. of Technology, Cambridge, MA, July 1998.

[34]Frech, M., and Zinner, T., "Concept of Wake Vortex Behaviour Classes," *Journal of Aircraft*, Vol. 41, No. 3, 2003, pp. 564–570.

[35]Frauenkron, H., Biegholdt, J., Maiss, M., Nalpanis, P., and Smith, E., "FLIP—Flight Performance Using Frankfurt ILS, A Statistical Evaluation of Navigational Performance of ILS-Approaches at Frankfurt International Airport," DFS German Air Navigation Services, Air Traffic Management Division, Offenbach, Germany, Feb. 2001.

[36]Hahn, K.-U., "Coping with Wake Vortex," International Congress of Aeronautical Sciences, ICAS 2002-7.3.1, Sept. 2002.

[37]Rossow, V. J., "Reduction of Uncertainties in Prediction of Wake-Vortex Locations," *Journal of Aircraft*, Vol. 39, No. 4, 2002, pp. 587–596.